Cloud-Gap Filtering for Reliable MSG-SEVIRI-Based Snow Cover Records

Semih Kuter [1], Çağrı Hasan Karaman [2], Mustafa Berkay Akpınar [2], Zuhal Akyürek [3,4]

[1] Çankırı Karatekin University, Faculty of Forestry, Dept. of Forest Engineering, Türkiye - semihkuter@karatekin.edu.tr
[2] HidroSAF Ltd., Middle East Technical University (METU) Technopolis, Türkiye - cagrikaraman@hidrosaf.com, berkay.akpinar@hidrosaf.com
[3] METU, Faculty of Engineering, Dept. of Civil Engineering, Türkiye - zakyurek@metu.edu.tr
[4] METU, Graduate School of Natural and Applied Sciences, Dept. of Geodetic and Geographic Information Technologies, Türkiye

Keywords: Snow cover, Cloud-gap filtering, MSG-SEVIRI, H SAF, Machine Learning.

Abstract

Snow cover is a key variable for climate monitoring and hydrological applications, yet optical satellite observations are strongly limited by cloud contamination, particularly during winter. The EUMETSAT H SAF H34 snow product derived from MSG-SEVIRI uses the unique 15-minute temporal resolution over the full SEVIRI disc to clear the clouds, but persistent clouds still cause substantial data gaps. In this study, we present a cloud-gap reconstruction framework that combines Numerical Weather Prediction data with machine learning to infer snow presence beneath cloud-covered pixels in the H34 product. Skin temperature, snow depth, and snow temperature fields from the Integrated Forecast System (IFS) were used as physically consistent predictors and resampled to the H34 grid, together with elevation information from SRTM.
An XGBoost-based model was trained using cloud-free H34 snow observations and applied exclusively to cloud-contaminated pixels to estimate the probability of underlying snow presence. Pixels exceeding an 80% probability threshold were reclassified as snow. The approach was applied to the winter seasons of 2024 and 2025 and validated over the European Alps using in-situ snow observations from World Meteorological Organization (WMO) stations. Evaluation using probability of detection (POD), false alarm ratio (FAR), and overall accuracy (ACC) shows a clear improvement in snow detection under cloudy conditions, with a significant reduction in missing observations. Compared to conventional temporal gap-filling methods, the proposed framework reduces reliance on temporal interpolation by directly exploiting physically meaningful meteorological information, while preserving the high temporal resolution advantage of MSG-SEVIRI.

1. Introduction

Snow cover is a key variable in the climate system, affecting the surface energy balance, water resources, and hydrological processes (Kuter *et al.*, 2018; Tekeli *et al.*, 2005). Reliable long-term records are necessary to support climate monitoring, numerical weather prediction, and hydrological modelling. Although optical sensors are the main tool for mapping snow, persistent cloud cover is the most significant limit for these products in the Northern Hemisphere (cf. Figure 1). Globally, clouds can hide more than 70% of the Earth's surface at any time, creating large data gaps that make daily satellite products less useful (Coll and Li, 2018; Yan and Zhang, 2025).

In Europe, cloud cover is very high during the winter season. For example, daily MODIS images in the Alps are often hidden by more than 60% cloud cover (Da Ronco and De Michele, 2014). The EUMETSAT Satellite Application Facility on Support to Operational Hydrology and Water Management (H SAF) provides several snow products. Among these, the H34 product (H-SAF_H34_PUM, 2023) provides a binary snow mask from the Spinning Enhanced Visible and Infrared Imager (SEVIRI) on geostationary satellites. This sensor has a spatial resolution of 3 km and a 15-minute repeat cycle, which is unique compared to polar-orbiting sensors. Daily composites from SEVIRI show 15–30% less cloud cover than MODIS over central Europe (Sürer *et al.*, 2014). However, clouds still reduce data availability in Northern Europe, limiting the use of these products in hydrological studies. Figure 1 illustrates the cloud contamination over the Pan-European region derived from the H SAF H10 binary snow mask product (H-SAF_H10_PUM, 2018), which is the predecessor of H34.

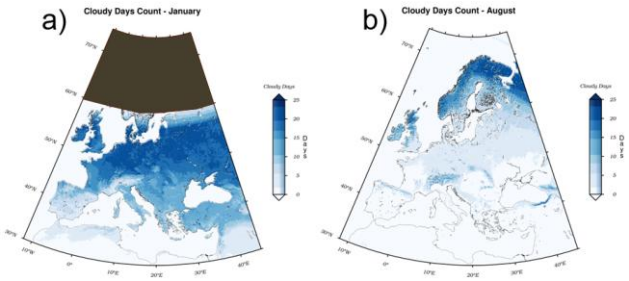

Figure 1. Cloudy days (a) in January (black shaded areas represent regions with missing data in January, caused by low solar illumination angles at high latitudes that prevent reliable snow detection.), and (b) in August obtained from H SAF H10 product (mean monthly values for 2012-2021).

To fix these gaps, cloud-gap-filling (CGF) techniques are used to estimate missing ground information (Deng *et al.*, 2024; Hall *et al.*, 2010). These methods typically use data from other sensors, spatial filters based on nearby pixels, or temporal interpolation using the most recent valid observation (MRVO) (Coll and Li, 2018; Deng *et al.*, 2024). Some advanced methods attempt to use both spatial and temporal information at the same

time to reach higher accuracy (Deng *et al.*, 2024; Hall *et al.*, 2010). However, traditional CGF strategies have several limits that affect the quality of the data. A major problem is that these methods often sacrifice spatial or temporal resolution to reach cloud-free coverage (Deng *et al.*, 2024; Gao *et al.*, 2011). Furthermore, the accuracy of a CGF decision depends on the "age" of the snow observation (Hall *et al.*, 2019; Hall *et al.*, 2010; Yuan *et al.*, 2022). As the number of days under clouds increases, the confidence in the reported state of the surface drops. This is a particular problem for surface features that change quickly (Hall *et al.*, 2010; Yuan *et al.*, 2022). Gap-filling can cause large errors during the beginning of snow accumulation or melting, when snow can appear or disappear in only one or two days (Gao *et al.*, 2011; Yuan *et al.*, 2022). Because of this, there is a need for better methods that can fill gaps while keeping uncertainty low in long-term climate records.

In this study, CGF is performed using a machine-learning-based reconstruction approach driven by physically consistent variables from the IFS (Buizza *et al.*, 2018), rather than conventional spatial or temporal interpolation techniques. Skin temperature, snow depth, and snow temperature fields, together with topographic variables derived from SRTM DEM are used to probabilistically infer snow presence beneath cloud-covered pixels in the MSG-SEVIRI H34 product. The methodology is applied to the winter seasons of 2024 and 2025 over the European Alps, and the reconstructed snow fields are evaluated using in-situ snow observations from WMO synoptic stations through standard binary performance metrics.

2. Data and Study Area

2.1 H SAF H34 Snow Product from MSG-SEVIRI

The H34 snow product provides daily binary snow cover information derived from visible and infrared radiometry (cf. Figure 2). Snow detection is based on a multispectral analysis of SEVIRI channels centred at 0.64, 1.6, 3.9, and 10.8 µm, which are selected to enhance the discrimination between snow, clouds, and snow-free surfaces under varying illumination and atmospheric conditions. The algorithm exploits the high reflectance of snow in the visible band, its distinct spectral behaviour at 1.6 µm, and thermal contrasts observed in the infrared channels for cloud detection and separation (H-SAF_H34_ATBD, 2020).

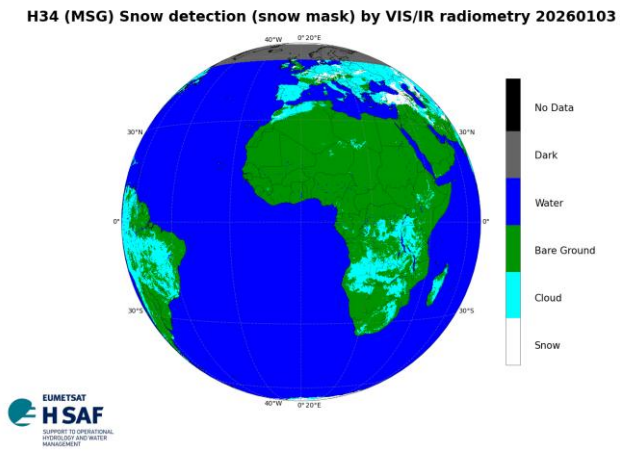

Figure 2. H SAF H34 product on 3 January 2026.

The H34 processing chain consists of two parallel algorithms optimised for flat/forested areas and mountainous regions, respectively. Instantaneous snow maps are first generated from 15-minute SEVIRI observations and subsequently combined through a multi-temporal analysis over a 24-hour window to maximise the retrieval of cloud-free snow information. The flat/forested and mountainous products are then merged using a predefined mountain mask to produce a single, spatially consistent snow mask covering the full MSG-SEVIRI disk. The final product classifies each pixel as snow, cloud, snow-free land, water, dark, or no-data, using cloud information from the Nowcasting Satellite Application Facility (NWC SAF) cloud products (Derrien, 2014), and includes quality flags describing product availability and merging status.

The native sampling of SEVIRI is approximately 3 km at the sub-satellite point, degrading to about 5 km over Europe due to viewing geometry. The merged H34 product is disseminated operationally via EUMETCast with a typical timeliness of approximately six hours after the end of the observation window. Despite its high temporal sampling, the H34 product remains affected by persistent cloud cover, particularly during winter and over northern and mountainous regions, resulting in spatially and temporally incomplete snow cover information.

2.2 Integrated Forecast System (IFS) and Auxiliary Data

Numerical Weather Prediction data from the IFS, operated by the European Centre for Medium-Range Weather Forecasts (ECMWF), were used as the primary auxiliary dataset for cloud-gap reconstruction. The IFS is a comprehensive global forecasting system that couples the atmosphere, land surface, ocean, sea ice, and wave components, and integrates a wide range of observations through advanced data assimilation techniques, including satellite radiances, radar measurements, radiosondes, and surface observations (Buizza *et al.*, 2018). This integrated framework ensures physical consistency among atmospheric and land-surface variables and provides robust representations of snow-related processes.

In this study, surface skin temperature, snow depth, and snow temperature fields from the IFS analysis at 12:00 UTC were selected as predictor variables due to their direct physical linkage to snow presence and surface conditions. These variables originate from the land surface and snow schemes embedded within the IFS and benefit from the continuous assimilation of multi-source observations, enhancing their reliability under cloud-covered conditions. The native spatial resolution of the IFS data (0.10°) was resampled to the MSG-SEVIRI H34 grid (approximately 3 km at nadir) using nearest-neighbour interpolation to ensure spatial consistency between datasets.

In addition to the IFS variables, topographic information was incorporated using elevation data from the Shuttle Radar Topography Mission (SRTM). Elevation was included as an auxiliary predictor to account for altitude-dependent snow processes and to improve the representation of snow variability in complex terrain, particularly in mountainous regions such as the European Alps.

2.3 Study Area and Temporal Coverage

The study was conducted over the European Alps, a region characterised by complex topography, strong elevation gradients, and pronounced seasonal snow dynamics. The Alps represent a challenging environment for optical snow cover retrieval due to frequent cloud cover, heterogeneous land surface conditions, and rapid snow accumulation and melt

processes (Hüsler *et al.*, 2014). At the same time, the region is of high relevance for hydrological applications, water resource management, and climate studies (Aili *et al.*, 2019; Vanham, 2012), making it well suited for evaluating cloud-gap reconstruction methods.

The analysis focused on selected winter and transitional months during the 2024 and 2025 seasons. Specifically, the study period includes January, February, March, April, May, November, and December of 2024, as well as January and February of 2025. This temporal coverage captures a wide range of snow conditions, including snow accumulation, peak snow extent, and melt phases, as well as periods with persistent cloud cover.

3. Methodology

3.1 Cloud-Gap Filling Concept

In this study, CGF is addressed through a physically constrained, machine-learning-based reconstruction framework rather than conventional spatial or temporal interpolation techniques. The objective is to infer snow presence beneath cloud-covered pixels in the H34 product by exploiting physically meaningful information from Numerical Weather Prediction data. The reconstruction is applied exclusively to pixels classified as cloud in the original H34 product, while cloud-free snow and no-snow observations are preserved unchanged. This strategy avoids altering reliable satellite observations and limits reconstruction uncertainty solely to cloud-contaminated areas.

3.2 Machine Learning Framework and the Predictor Variables

A gradient-boosted decision tree model based on XGBoost was used to establish statistical relationships between the selected variables and observed snow cover. XGBoost (Chen and Guestrin, 2016) is a gradient boosting decision tree algorithm designed to provide high predictive performance, robustness, and computational efficiency. By iteratively combining weak learners and optimising a regularised objective function, XGBoost effectively captures non-linear relationships between predictor variables and target classes. Its ability to handle heterogeneous inputs and to provide probabilistic outputs makes it well suited for environmental applications involving complex surface processes and uncertain observations (Niazkar *et al.*, 2024).

Cloud-free pixels from the H34 product were used as reference data to train the model, ensuring consistency between the satellite observations and the learning target. The dataset was randomly split into training (80%) and testing (20%) subsets. Model hyperparameters were optimised with a specific emphasis on maximising snow detection recall, reflecting the primary objective of recovering snow information under cloud-covered conditions. The trained model outputs the probability of snow presence for each input pixel, allowing a probabilistic interpretation of the reconstruction results.

The reconstruction framework relies on variables derived from the IFS analysis at 12:00 UTC. Skin temperature, snow depth, and snow temperature were selected as predictor variables due to their direct physical relationship with snow presence and surface conditions. These variables originate from the land surface and snow schemes embedded within the IFS and benefit from continuous multi-source data assimilation. In addition, SRTM elevation data were included to account for altitude-dependent snow processes. All predictor variables were resampled to the MSG-SEVIRI H34 grid using nearest-neighbour interpolation to ensure spatial consistency between datasets.

The trained XGBoost model outputs the probability of snow presence for each cloud-contaminated pixel. A probability threshold of 0.80 was applied, and pixels with estimated probabilities exceeding this threshold were reclassified as snow.

3.3 Validation Strategy and Performance Metrics

The performance of the reconstructed snow cover product was evaluated using in-situ snow observations from WMO synoptic stations over the European Alps. A snow depth (SD) threshold of 5 cm was applied to station measurements to define snow presence. Then, a binary confusion matrix framework (cf. Table 1) was employed to compare the original and reconstructed H34 products against the reference observations. Standard performance metrics, including POD (i.e., A/(A+C)), FAR (i.e., B/(A+B)), and ACC (i.e., (A+D)/(A+B+C+D)), were computed to quantify improvements in snow detection under cloudy conditions and to assess potential trade-offs introduced by the CGF process.

		Ground Truth (in-situ SD)	
		Snow	**No Snow**
Satellite Product (H34)	**Snow**	HITS (A)	FALSE ALARMS (B)
	No Snow	MISSES (C)	CORRECT NEGATIVES (D)

Table 1. Binary error matrix.

4. Results

4.1 Overall Impact of the Cloud-Gap Reconstruction

The application of the XGBoost-based CGF leads to a clear and systematic improvement in the snow detection performance of the MSG-SEVIRI H34 product. Compared to the original H34, the reconstructed product shows a consistent increase in snow detection skill across all analysed months (cf. Figure 3). This improvement is reflected by higher POD and ACC, while FAR remains stable overall and even slightly decreases when aggregated over the full period.

4.2 Behaviour of the Confusion Matrix Components and Improvement in Snow Detection Performance

A consistent and robust pattern is observed in the elements of the updated binary confusion matrix presented in Table 2. For all analysed months, the numbers of misses (C) and correct negatives (D) remain unchanged between the original H34 product, and the reconstructed product obtained using the CGF approach. In contrast, the number of hits (A) increases systematically after applying the CGF procedure, accompanied by a limited increase in false alarms (B). This behaviour directly reflects the design of the reconstruction framework. The XGBoost model is applied exclusively to pixels originally classified as cloud in the H34 product, while all cloud-free snow and no-snow pixels are preserved. Consequently, the

reconstruction can only convert cloud pixels into snow, leading to an increase in correctly detected snow cases (A) when snow is present and to a moderate increase in false snow detections (B) when snow is absent. The unchanged values of C and D provide strong evidence that the proposed method does not modify reliable cloud-free classifications and does not introduce additional missed snow cases.

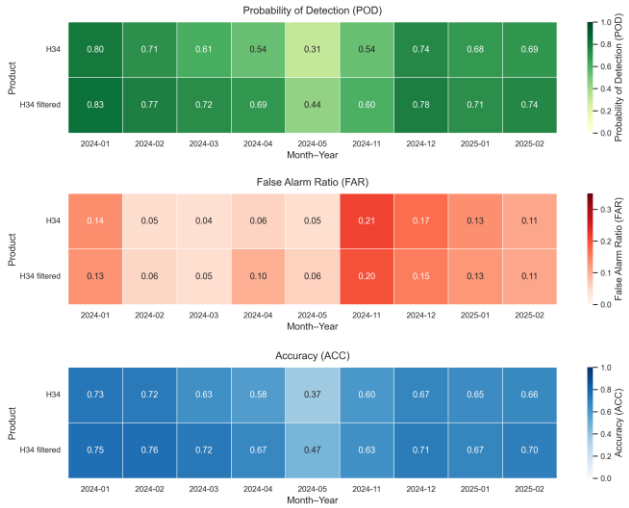

Figure 3. Performance metrics of the original H34 and the CGF H34 products.

The increase in hits (A) is directly reflected in higher POD values for the reconstructed H34 product. When aggregated over all analysed months, POD increases from 0.678 for the original H34 product to 0.735 for the reconstructed product. This improvement confirms the ability of the CGF approach to recover snow information obscured by cloud cover. The most pronounced gains are observed during months characterised by active snow accumulation and melt, with monthly POD increases reaching up to +0.15, highlighting conditions under which conventional cloud-gap-filling approaches based on temporal interpolation are known to perform poorly.

Original H34						
Year and Month	**A**	**B**	**C**	**D**	**No. of Data**	**No. of Stations**
2024-1	761	121	193	88	1,934	153
2024-2	327	16	132	47	973	80
2024-3	213	10	136	36	823	84
2024-4	172	11	148	46	879	89
2024-5	63	3	141	22	472	34
2024-11	164	44	141	112	735	135
2024-12	602	125	217	106	1,680	133
2025-1	603	94	280	83	1,680	124
2025-2	337	41	152	33	964	99
CFG H34						
2024-1	934	140	193	88	1,934	153
2024-2	445	26	132	47	973	80
2024-3	356	17	136	36	823	84
2024-4	324	36	148	46	879	89
2024-5	109	7	141	22	472	34
2024-11	212	52	141	112	735	135
2024-12	751	137	217	106	1,680	133
2025-1	702	102	280	83	1,680	124
2025-2	437	53	152	33	964	99

Table 2. Monthly confusion matrix components for the original H34 and the cloud-gap-filled H34.

Although FAR exhibits small month-to-month variations, the overall impact remains limited. When aggregated over the full study period, FAR slightly decreases from 0.125 to 0.118, indicating that the gain in snow detection is not accompanied by a substantial increase in false snow assignments. This balance is further reflected in the improvement of ACC, which increases from 0.655 to 0.697. The conservative probability threshold of 0.80 plays a key role in maintaining this balance by favouring robust snow detection under uncertain conditions.

The performance gains achieved by the CGF approach are particularly evident during transitional periods, when snow cover is spatially heterogeneous and cloud persistence is high. During these months, the reconstructed product exhibits a marked reduction in missing snow observations, while maintaining stable performance during mid-winter conditions. This behaviour highlights the capacity of the proposed framework to adapt to varying snow and meteorological regimes by exploiting physically consistent information from Numerical Weather Prediction data, rather than relying on assumptions of temporal persistence.

A direct comparison between the original and reconstructed H34 products confirms that the improvements are confined to cloud-contaminated regions (cf. Figure 4). Cloud-free observations remain unchanged, ensuring that the intrinsic quality of the original satellite retrievals is preserved. This targeted reconstruction strategy enhances the spatial completeness of the H34 snow product while maintaining its original temporal resolution and observational integrity.

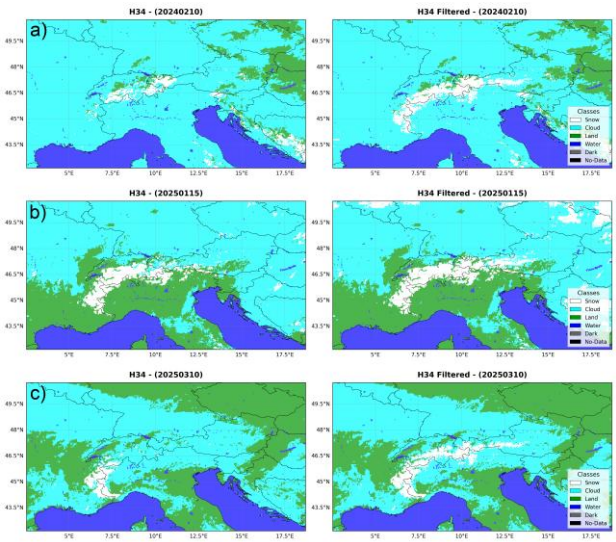

Figure 4. Visual comparison between H34 and CGF H34 on: a) 10 Feb 2024, b) 15 Jan 2025, and c) 10 Mar 2025.

4.3 XGBoost Variable Importance Scores

To interpret the contribution of individual predictor variables and to improve the transparency of the machine-learning model, Shapley Additive Explanations (SHAP) (Lundberg and Lee, 2017) were employed. SHAP provides a consistent framework to quantify the influence of each input variable on the model output by attributing the prediction to individual features in a game-theoretic sense. This allows both the relative importance of predictors and the direction of their effects on snow probability to be examined.

The SHAP analysis (cf. Figure 5) reveals that skin temperature is the dominant predictor controlling the model output, with lower skin temperature values strongly increasing the probability of snow presence, while higher values have a suppressing effect. Elevation emerges as the second most influential variable, indicating a clear orographic control on snow occurrence. SD from the IFS contributes positively to snow detection but with a narrower impact range, suggesting a supportive rather than dominant role. Latitude and snow temperature provide additional climatic and thermodynamic context, whereas longitude shows only a marginal contribution. Overall, the SHAP results demonstrate that the XGBoost model relies on physically consistent variables and relationships, reinforcing the interpretability and robustness of the proposed cloud-gap reconstruction framework.

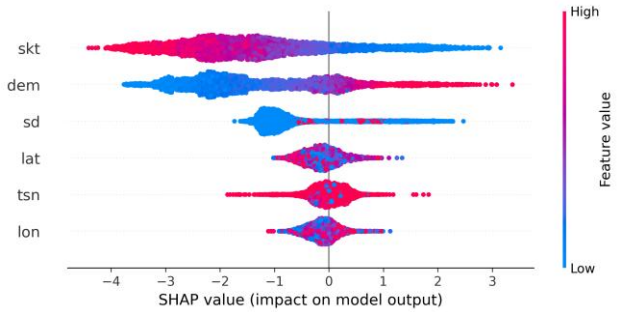

Figure 5. SHAP values for the developed XGBoost model (skt: skin temperature, dem: elevation, sd: snow depth, lat: latitude, tsn. snow temperature, and lon: longitutude).

5. Conclusions and Outlook

This study presents a physically consistent, machine-learning-based cloud-gap reconstruction framework to enhance the MSG-SEVIRI H34 snow cover product under persistent cloud conditions. By integrating variables from the Integrated Forecast System with an XGBoost model, snow presence beneath cloud-covered pixels was probabilistically inferred without modifying cloud-free satellite observations.

Validation against in-situ SD measurements demonstrates a clear improvement in snow detection performance. The reconstructed product shows a systematic increase in POD and ACC, while changes in FAR remain limited. The characteristic behaviour of the confusion matrix, with unchanged misses and correct negatives and increased hits, confirms that the improvements are confined to cloud-contaminated pixels and are consistent with the design of the reconstruction approach.

The SHAP analysis provides further insight into the model behaviour and supports its physical interpretability. Skin temperature and elevation emerge as the dominant predictors, followed by snow depth, while latitude and snow temperature play secondary roles. This ranking is physically meaningful and demonstrates that the model relies on coherent thermodynamic and topographic controls rather than spurious correlations.

Overall, the proposed framework improves the spatial completeness of the H34 snow product while preserving its native temporal resolution and observational integrity. The results highlight the potential of combining Numerical Weather Prediction data with explainable machine-learning techniques to address cloud-related limitations in geostationary snow products and to support hydrological and climate-oriented applications.

Future work will focus on extending the analysis to additional regions, including Türkiye, Georgia, and the Tatra Mountains, and on performing validation over longer time periods. This will allow a more comprehensive assessment of the robustness and transferability of the proposed approach under different climatic, topographic, and snow regime conditions.

References

Aili, T., Soncini, A., Bianchi, A., Diolaiuti, G., D'Agata, C. and Bocchiola, D. (2019). Assessing water resources under climate change in high-altitude catchments: a methodology and an application in the Italian Alps. *Theoretical and Applied Climatology,* 135(1), pp. 135-156.

Buizza, R., Balmaseda, M. A., Brown, A., English, S., Forbes, R., Geer, A., Haiden, T., Leutbecher, M., Magnusson, L., Rodwell, M., Sleigh, M., Stockdale, T., Vitart, F. and Wedi, N. (2018). The development and evaluation process followed at ECMWF to upgrade the Integrated Forecasting System (IFS). *ECMWF Technical Memoranda.* Retrieved on 1 January 2026, from https://www.msleigh.io/pubs/The_development_and_evaluation_process_followed_at_ECMWF_to_upgrade_the_IFS.pdf.

Chen, T. and Guestrin, C. (2016). *XGBoost: A Scalable Tree Boosting System*. Paper presented at the Proceedings of the 22nd ACM SIGKDD International Conference on Knowledge Discovery and Data Mining, San Francisco, California, USA. https://doi.org/10.1145/2939672.2939785

Coll, J. and Li, X. (2018). Comprehensive accuracy assessment of MODIS daily snow cover products and gap filling methods. *ISPRS Journal of Photogrammetry and Remote Sensing,* 144, pp. 435-452.

Da Ronco, P. and De Michele, C. (2014). Cloud obstruction and snow cover in Alpine areas from MODIS products. *Hydrol. Earth Syst. Sci.,* 18(11), pp. 4579-4600.

Deng, G., Tang, Z., Dong, C., Shao, D. and Wang, X. (2024). Development and Evaluation of a Cloud-Gap-Filled MODIS Normalized Difference Snow Index Product over High Mountain Asia. *Remote Sensing,* 16(1), pp. 192.

Derrien, M. (2014). NWC SAF Product User Manual for "Cloud Products" (CMa-PGE01 v3.2, CTPGE02 v2.2 & CTTH-PGE03 v2.2). Retrieved on 13 February 2025, from https://www.nwcsaf.org/AemetWebContents/ScientificDocumentation/Documentation/MSG/SAF-NWC-CDOP2-MFL-SCI-PUM-01_v3.2.3.pdf.

Gao, Y., Lu, N. and Yao, T. (2011). Evaluation of a cloud-gap-filled MODIS daily snow cover product over the Pacific Northwest USA. *Journal of Hydrology,* 404(3), pp. 157-165.

H-SAF_H10_PUM. (2018). Product User Manual (PUM) for product H10 – SN-OBS-1 Snow detection (snow mask) by VIS/IR radiometry. *EUMETSAT Satellite Application Facility on Support to Operational Hydrology and Water Management.* Retrieved on 13 February, 2025, from https://hsaf.meteoam.it/Products/Detail?prod=H10.

H-SAF_H34_ATBD. (2020). Algorithm Theoretical Baseline Document (ATBD) for product H34 – SE-D-SEVIRI Snow detection (snow mask) by VIS/IR radiometry. *EUMETSAT*

Satellite Application Facility on Support to Operational Hydrology and Water Management. Retrieved on 13 February, 2025, from https://hsaf.meteoam.it/Products/Detail?prod=H34.

H-SAF_H34_PUM. (2023). Product User Manual (PUM) for product H34 – SN-OBS-1G Snow detection (snow mask) by VIS/IR radiometry. *EUMETSAT Satellite Application Facility on Support to Operational Hydrology and Water Management.* Retrieved on 13 February, 2025, from https://hsaf.meteoam.it/Products/Detail?prod=H34.

Hall, D. K., Riggs, G. A., DiGirolamo, N. E. and Román, M. O. (2019). Evaluation of MODIS and VIIRS cloud-gap-filled snow-cover products for production of an Earth science data record. *Hydrol. Earth Syst. Sci.,* 23(12), pp. 5227-5241.

Hall, D. K., Riggs, G. A., Foster, J. L. and Kumar, S. V. (2010). Development and evaluation of a cloud-gap-filled MODIS daily snow-cover product. *Remote Sensing of Environment,* 114(3), pp. 496-503.

Hüsler, F., Jonas, T., Riffler, M., Musial, J. P. and Wunderle, S. (2014). A satellite-based snow cover climatology (1985–2011) for the European Alps derived from AVHRR data. *The Cryosphere,* 8(1), pp. 73-90.

Kuter, S., Akyurek, Z. and Weber, G. W. (2018). Retrieval of fractional snow covered area from MODIS data by multivariate adaptive regression splines. *Remote Sensing of Environment,* 205, pp. 236-252.

Lundberg, S. M. and Lee, S.-I. (2017). A Unified Approach to Interpreting Model Predictions. In I. Guyon, U. V. Luxburg, S. Bengio, H. Wallach, R. Fergus, S. Vishwanathan and R. Garnett (Eds.), *Advances in Neural Information Processing Systems* (Vol. 30): Curran Associates, Inc.

Niazkar, M., Menapace, A., Brentan, B., Piraei, R., Jimenez, D., Dhawan, P. and Righetti, M. (2024). Applications of XGBoost in water resources engineering: A systematic literature review (Dec 2018–May 2023). *Environmental Modelling & Software,* 174, pp. 105971.

Sürer, S., Parajka, J. and Akyürek, Z. (2014). Validation of the operational MSG-SEVIRI snow cover product over Austria. *Hydrology and Earth System Sciences,* 18(2), pp. 763-774.

Tekeli, A. E., Akyürek, Z., Şorman, A. A., Şensoy, A. and Şorman, Ü. (2005). Using MODIS snow cover maps in modeling snowmelt runoff process in the eastern part of Turkey. *Remote Sensing of Environment,* 97, pp. 216-230.

Vanham, D. (2012). The Alps under climate change: implications for water management in Europe. *Journal of Water and Climate Change,* 3(3), pp. 197-206.

Yan, D. and Zhang, Y. (2025). Investigating snow cover duration changes based on a cloud-free snow cover product developed using a spatiotemporal cloud removal method for Northeast China. *International Journal of Digital Earth,* 18(1), pp. 2497520.

Yuan, Y., Li, B., Gao, X., Liu, W., Li, Y. and Li, R. (2022). Validation of Cloud-Gap-Filled Snow Cover of MODIS Daily Cloud-Free Snow Cover Products on the Qinghai–Tibetan Plateau. *Remote Sensing,* 14(22), pp. 5642.